AD NUMBER

AD852770

LIMITATION CHANGES

TO:

Approved for public release; distribution is unlimited.

FROM:

Distribution authorized to U.S. Gov't. agencies and their contractors; Critical Technology; 24 APR 1969. Other requests shall be referred to U.S. Naval Ordnance Laboratory, White Oak, Silver Spring, MD 20910. This document contains export-controlled technical data.

AUTHORITY

NOL ltr dtd 15 Nov 1971

NOLTR 69-84

STRUCTURAL ANALYSIS OF NOL EXPLOSION TESTING FACILITIES

By
James F. Proctor

24 APRIL 1969

NOL
UNITED STATES NAVAL ORDNANCE LABORATORY, WHITE OAK, MARYLAND

NOLTR 69-84

STRUCTURAL ANALYSIS OF NOL EXPLOSION TESTING FACILITIES

Prepared by:
James F. Proctor

ABSTRACT: Installation of a heavy steel door in the labyrinth passageway of existing Naval Ordnance Laboratory (NOL) explosion testing facilities (bombproofs) is shown to reduce drastically the transmitted airblast pressure outside the building. Completely enclosing an explosion in this manner has caused concern for the structural capability of the bombproofs to withstand both the shock pressures and long duration gas pressures on a continuous use basis. This report presents an experimental and analytical study of the structural response of a typical bombproof to contained and vented explosions. It shows that the maximum deflections and stresses in the building are not significantly altered by completely enclosing the explosion. Experimental blast and response data are presented and compared with analytical predictions.

PUBLISHED 24 APRIL 1969

U. S. NAVAL ORDNANCE LABORATORY
WHITE OAK, MARYLAND

NOLTR 69-84 24 April 1969

STRUCTURAL ANALYSIS OF NOL EXPLOSION TESTING FACILITIES

The work described in this report was performed at the request of the management at the U. S. Naval Ordnance Laboratory. It was known that the installation of a heavy steel door in existing explosion testing facilities at NOL significantly reduced the transmitted airblast pressure outside the building and eliminated noise complaints from neighboring home owners. However, there was concern that the total confinement of an explosion in these facilities on a continuous use basis would produce an undesirable and possibly unsafe loading condition that could exceed the structural capability of these structures. An experimental and analytical study was performed that shows the structural integrity of the buildings is not endangered by the total containment of test explosions.

The mention of names of proprietary products in this report constitutes neither an endorsement nor criticism of these products by the United States Government or by the U. S. Naval Ordnance Laboratory.

The author expresses grateful appreciation to the following persons who donated their time, instrumentation, and facilities in the conduct of the experimental program: W. Anderson, J. Berman, R. Huff, B. Lancaster, L. Sadwin, and M. Swisdak of the Air/Ground Explosions Division; E. Duck, D. Gilmore, L. Roslund, and F. Ruggeri of the Explosions Dynamics Division. Also appreciation goes to R. Larson and D. Lehto of the Air/Ground Explosions Division for their help in computer calculations.

E. F. SCHREITER
Captain, USN
Commander

C. J. ARONSON
By direction

CONTENTS

ILLUSTRATIONS

CONTENTS (Cont'd)

TABLES

INTRODUCTION

Currently at the Naval Ordnance Laboratory, the amount of explosive that can be fired in the existing heavy-duty explosion test facilities (bombproofs) such as Buildings 314 and 324 is limited to an equivalence of 5 pounds of TNT. From past experience it is believed that this limit is the safe maximum in terms of building structural capability for repeated and continuous use. However, on certain days of adverse weather conditions, complaints of excessive noise and vibration from neighboring private homes have been received. To eliminate this problem, firing limits of $\frac{1}{2}$-lb TNT equivalent in a bombproof have been imposed when any of the following conditions exist:

1. Wind velocity is equal to or greater than 15 mph.
2. Positive temperature gradient exists or a negative temperature gradient is less than $\frac{1}{2}^{\circ}$F/100 ft. (Temperature readings are taken at ground level and at 100 ft.)

In many cases these conditions severely impede the progress of a concentrated firing program.

One bombproof, Building 324, has been modified with a heavy steel door to completely close the bombproof. From preliminary tests conducted in past years, it appeared that the door closure reduced the noise and pressures external to the bombproof so significantly that, at present, charges up to 5-lb TNT equivalent can be fired in this closed bombproof irrespective of weather conditions. However, because of minor inconveniences in test procedure and some concern for the structural capability of the building to withstand the completely enclosed explosion, the door is only used when adverse weather conditions exist. For these reasons doors on other bombproofs at the Laboratory have not been installed.

The detonation of an explosive charge in an enclosed space produces two potentially destructive mechanisms, the shock loadings with subsequent reflections and the quasi-static equilibrium gas pressure. Bombproofs at the Laboratory, such as Buildings 314 and 324, have been subjected to 5-lb explosive detonations over a period of many years; however, the buildings have been vented through existing passageways allowing a rather rapid decay of the gas pressure. Because of the venting, it has been assumed that response of the building walls to shock loading was the sole criteria for establishing safe firing limits. Since no severe damage

to the building walls has been noted after years of use at the 5-lb level, the 5-lb safe limit has been established on experience.

The incorporation of a door to completely enclose the explosion makes it mandatory that the building withstand the gas pressure in addition to the shock loading. Although in limited use the closure of the door has not produced any notable damage to the building walls, there is concern as to the building capabilities under continuous 5-lb firings with the door completely closed. This leads to the objectives of this report; they are to determine analytically and/or experimentally

1. the external pressure transmitted outside the building as a function of vent area
2. the internal shock loading on the building walls
3. the internal gas pressure and its rate of decay with varying vent areas
4. the structural response of the building walls to the internal explosion loadings.

DESCRIPTION OF A BOMBPROOF

A typical bombproof such as Building 324 is shown in Figure 1 with appropriate dimensions. The actual test chamber is 10' x 15' x $8\frac{1}{2}$' with three view ports for camera observation. The walls of the test chamber are protected from fragments by 1-in armor plate backed with $1\frac{5}{8}$-in wood as shown in Figure 2. A 4-ft wide labyrinth leading out of the test chamber prevents fragments and blast from having a direct path to the outside. The heavy steel door in the labyrinth closes a 16.6-ft^2 vent area and encloses a total internal building volume of 2,010 ft^3.

All walls, ceiling, and flooring in the test chamber are 2-ft thick reinforced concrete with a compressive strength of about 3,000 psi. Typical corner and wall reinforcing are shown in Figure 2. Steel bars $\frac{3}{4}$-in diameter on 8-in centers running vertically and horizontally from a reinforcing grid a minimum of 3 inches below both the internal and external wall surfaces. Steel bars $\frac{1}{2}$-in diameter on 16-in centers tie these two grids together. At a corner the outside reinforcing bars overlap for a distance of 4 feet from the corner. Also in a corner $\frac{3}{4}$-in diameter, 45-in long stirrups are placed on 8-in centers to prevent corner cracks from propagating through the wall.

An inspection of the concrete walls in Building 324 revealed the following items concerning wall cracks:

1. Nearly all cracks on the outside vertical surface originate in the mid-height region and propagate horizontally.
2. Most of the above cracks are of the hairline variety; however, a few are through-cracks and some are as much as $\frac{1}{16}$-in wide. These wide cracks actually breathe when a confined explosion occurs in the bombproof. The escape of the high pressure explosion gases through these cracks and the associated erosion effects could easily account for the size of these cracks.
3. No cracks were found on the outside surface near a corner.
4. The inside surface of the concrete walls are covered with armor plate thereby making an adequate inspection impossible. However, in a few places at corners, a sufficient gap in the plating exists to allow the observation of a hairline crack directly in the corner apparently propagating along the joint.

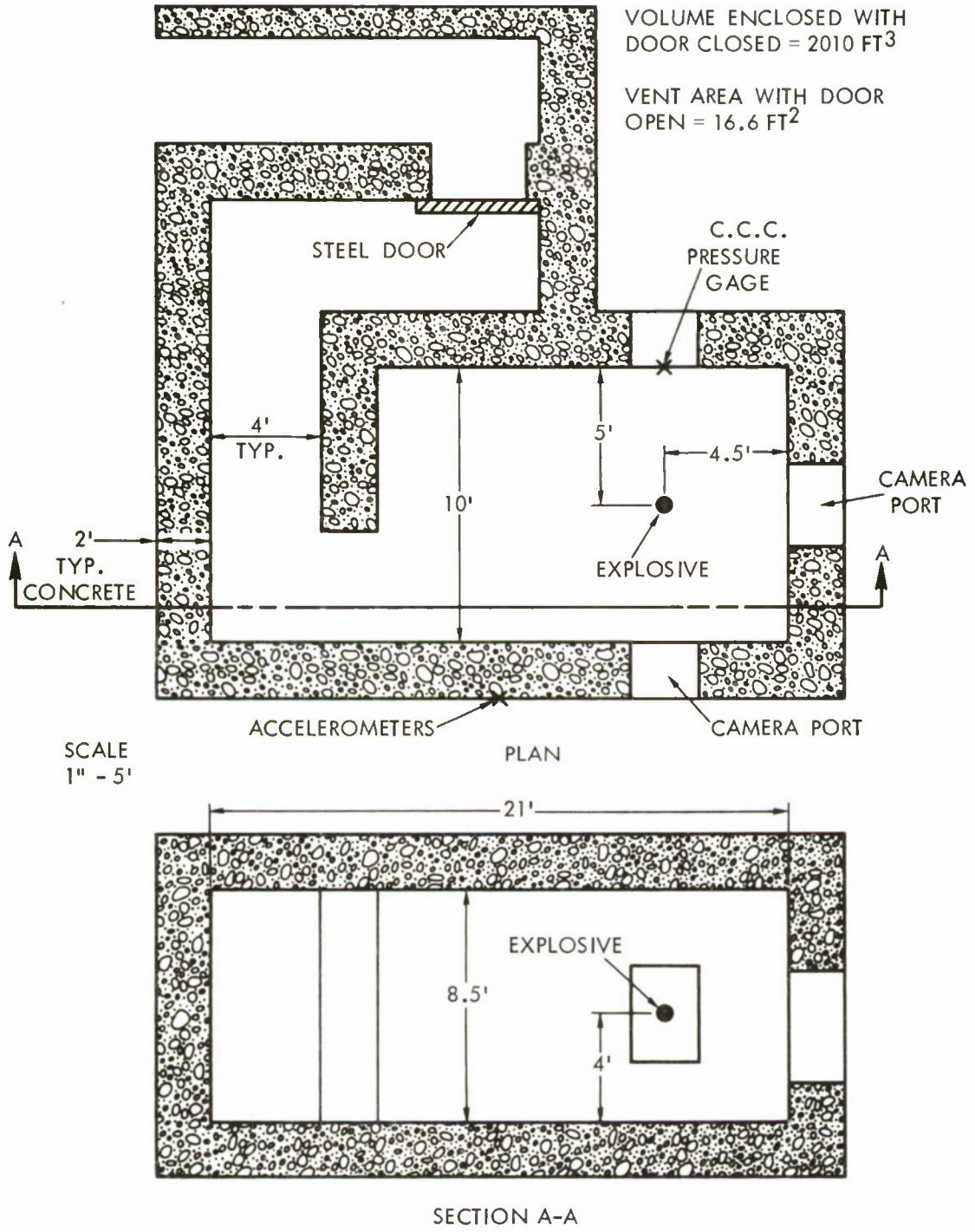

FIG. 1 CONFIGURATION OF TYPICAL BOMBPROOF

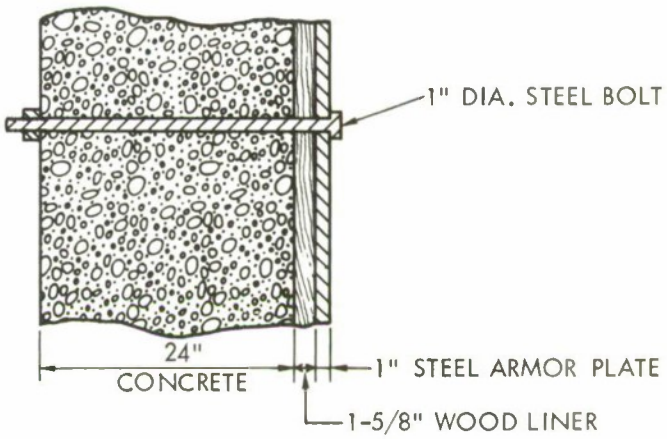

TYPICAL WALL WITH WOOD LINER AND ARMOR PLATE

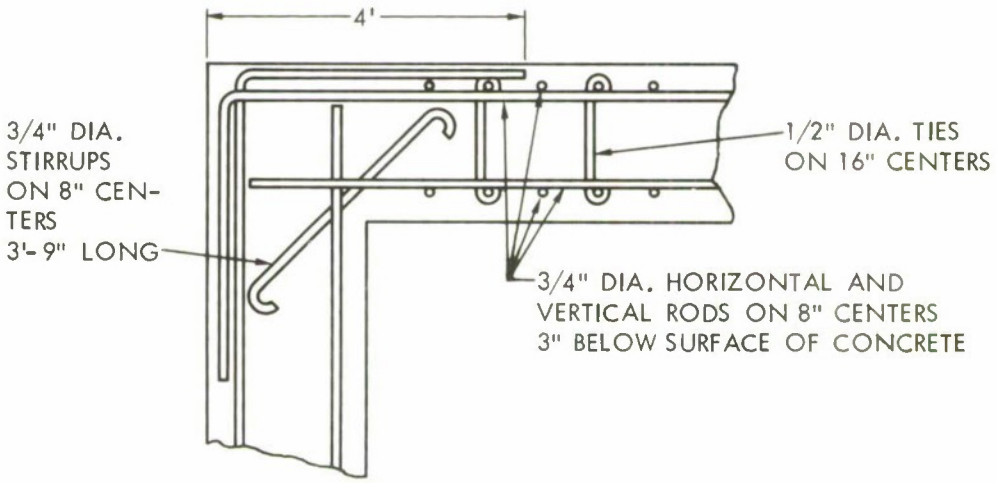

TYPICAL CORNER AND WALL REINFORCING

FIG. 2 CONSTRUCTION DETAILS

EXPERIMENTAL PROGRAM

A brief experimental program was conducted in Building 324 to provide some basic data on the internal wall pressure loading, wall frequency response, and outside pressure levels. Charge weights of 1, 2, and 5 lb of pentolite located in line with the side ports (4.5 ft from front wall, 5 ft from side ports, and 4 ft above floor -- see Figure 1) were fired in the test chamber. Gas vent area was varied by opening or closing the heavy steel door in the labyrinth passageway.

It was believed impossible to obtain meaningful shock loading pressure on the wall at a single gage point and multi-point measurements were deemed too expensive. Therefore, only the equilibrium gas pressure in the chamber was recorded. This pressure was measured with a Consolidated Controls Corporation variable reluctance pressure gage mounted in one of the wall viewing ports (see Figure 1) and recorded on a conventional oscilloscope. Airblast pressures transmitted outside the bombproof were measured with Atlantic Research Corporation LC-33 piezoelectric pencil gages and General Radio Corporation sound level meters Type 1551A and B equipped with an impact noise analyzer Type 1556A. The LC-33 gages were used with an NOL developed high-input resistance amplifier and a standard oscilloscope. Locations of these gages are shown in Figure 3.

Three accelerometers Endevco Model 2213 were mounted in a cluster located on the outside surface approximately at the center of the long 21-ft concrete wall (see Figure 1). These accelerometers were used with an Endevco Model 2712A charge amplifier powered by an Endevco Model 2627A power supply and recorded on conventional oscilloscopes.

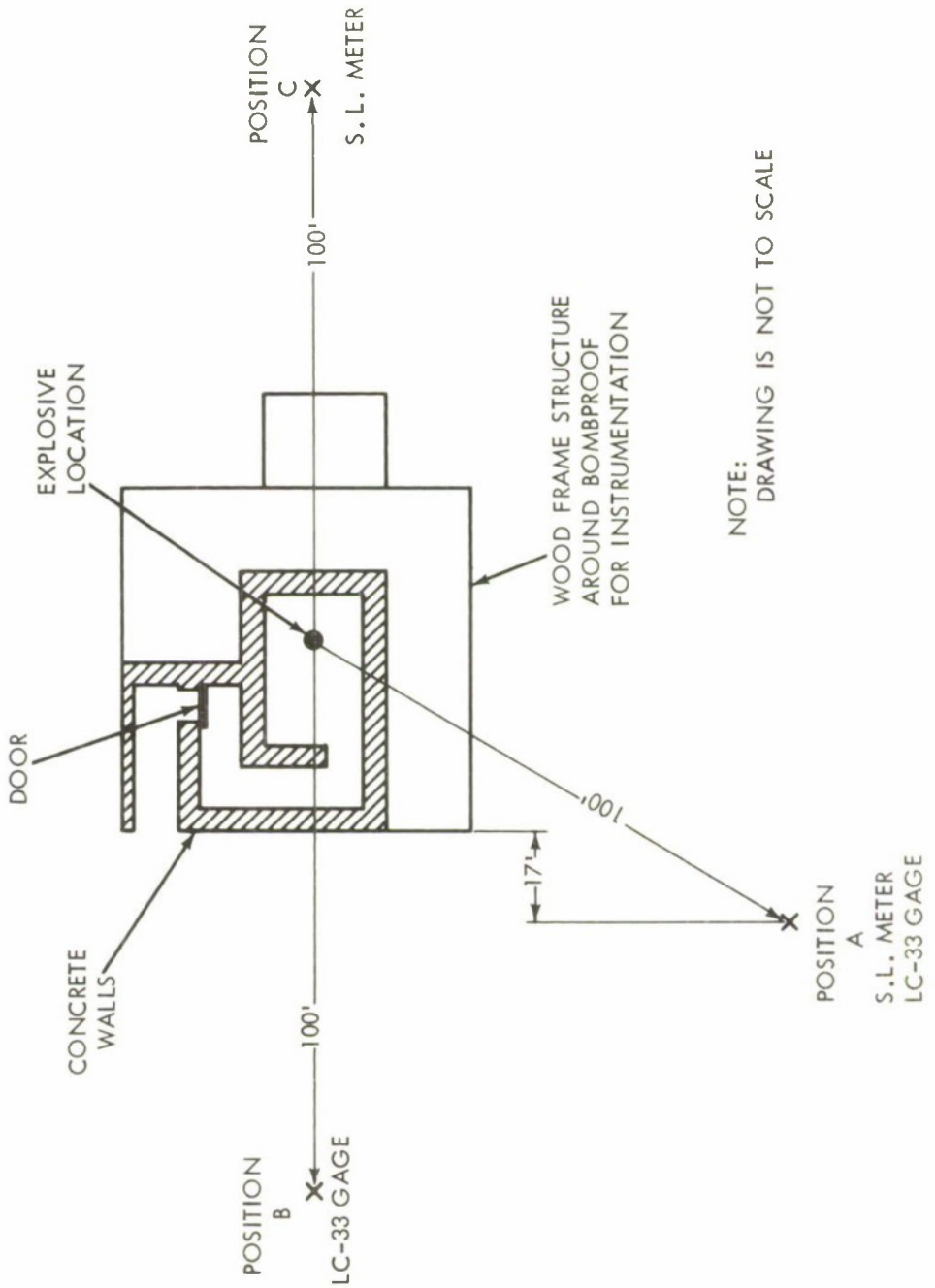

FIG. 3 LOCATION OF OUTSIDE SOUND AND PRESSURE GAGES

EXPERIMENTAL AND ANALYTICAL RESULTS

Test specifications and experimental results for thirteen explosion tests are presented in tabular form in Tables 1 and 2.

External Pressures. The reduction in external blast pressures outside the building for the various degrees of chamber venting is shown in Figure 4. Only the data obtained from the pencil gages are plotted because the sound level meter measurements (1) were always lower than the pressures recorded by the pencil gages and (2) were inconsistent and widely varying to the point that all sound level data were questionable. It is noted from the curves that the pencil gage data are self consistent and that there is little difference in the pressure levels at Stations A and B. Plotted in this figure for comparison purposes is the peak pressure curve for hemispherical TNT surface explosions for unconfined space from reference (1). It can be determined that a 5-lb pentolite charge fired with the door fully open produces approximately the same peak pressure at the 100-ft distance as a 1-lb TNT charge fired unconfined at ground level. Also a $\frac{1}{2}$-lb pentolite charge for the open door condition (limit for bad weather conditions) produces about the same pressure as an unconfined 6-gm TNT charge at ground level. From the curves it is seen that a 5-lb pentolite shot with the door completely closed will produce a lower pressure than a $\frac{1}{2}$-lb charge with the door open, and the pressure is equivalent to about a 1.5-gm TNT charge fired unconfined at ground level for the 100-ft distance.

An interesting observation not reflected in Table 1 was made from the actual pressure-time traces from the pencil gages. In all cases where the chamber was completely open, a steep-front shock was recorded. However, for the partially closed (2.4-ft^2 vent area) and the fully closed door conditions, there was a definite rise time associated with the peak pressure. For example, a rise time of approximately 6 milliseconds was recorded for a 5-lb shot with the door partially open, and a 9-millisecond rise time for the same charge with the door completely closed. The total positive pressure duration was about 13 milliseconds for both of these conditions as compared to about 10 milliseconds for the 5-lb shot, open door condition. Apparently the observed finite pressure rise-time for the restricted vent areas was the result of wall motion, slow sustained venting, and pressure levels too low (0.07 psi or less) to shock up at the 100-ft distance.

TABLE 1 - OUTSIDE SOUND AND PRESSURE MEASUREMENTS

TEST NO.	CHARGE WEIGHT (LB)	VENT AREA (FT^2) [1]	λ [2] (FT/LB$^{1/3}$)	ΔT [3] (°F)	WIND SPEED/DIR. (MPH/DIR.)	STATION A			STATION B	STATION C	
						SLM (dB)	SLM (PSIG)	LC-33 (PSIG)	LC-33 (PSIG)	SLM (dB)	SLM (PSIG)
1	1	16.6	100	-3.6	1/S	130	0.0093	-	-	130	0.0093
2	1	16.6	100	-2.8	1/NW	>120	>0.0029	0.0751	0.0836	130	0.0093
3	1	2.4	100	-3.6	0	129	0.0083	0.0180	0.0216	124	0.0047
4	1	0	100	-3.5	1/NE	123	0.0042	0.0054	0.0059	112	0.0016
5	2	16.6	79.4	-4.0	1/NW	136	0.0175	0.1950	0.1490	135	0.0165
6	2	2.4	79.4	-3.8	1/NE	135	0.0165	0.0270	0.0324	127	0.0068
7	2	0	79.4	-3.6	0	>120	>0.0029	0.0120	0.0135	118	0.0024
8	5	16.6	58.4	-4.0	0	139	0.0260	0.2760	0.3510	139	0.0260
9	5	16.6	58.4	-3.6	1/NE	147	0.0625	0.2760	0.3510	142	0.0370
10	5 [4]	16.6	58.4	-3.6	0	>150	>0.0930	0.3000	0.3370	139	0.0260
11	5	2.4	58.4	-3.8	1/E	139	0.0260	0.0600	0.0676	131	0.0105
12	5	1.2 [5]	58.4	-3.8	2/SSE	132	0.0117	0.0270	0.0216	124	0.0047
13	5	0	58.4	-5.0	1/NE	125	0.0052	0.0240	0.0243	125	0.0052

NOTES:
1. DOOR COMPLETELY OPEN FOR VENT AREA OF 16.6 FT^2; COMPLETELY CLOSED FOR 0 FT^2.
2. GAGE DISTANCE WAS 100 FT.
3. ΔT EQUALS TEMPERATURE AT TOP OF 100' TOWER AT BLDG. 309 MINUS TEMPERATURE AT GROUND LEVEL.
4. NEIGHBOR COMPLAINED ON THIS TEST FIRING.
5. VENT AREA UNCERTAIN BECAUSE OF DOOR DAMAGE.

TABLE 2 - INTERNAL PRESSURE, VENT TIME, AND ACCELERATION MEASUREMENTS

TEST NO.	CHARGE WEIGHT (LB)	VENT AREA (FT^2) [1]	PEAK GAS PRESSURE (PSIG)	VENT TIME (SEC)	WALL FREQUENCY			PEAK WALL ACCELERATION		
					GAGE 1 (Hz)	GAGE 2 (Hz)	GAGE 3 (Hz)	GAGE 1 (G's)	GAGE 2 (G's)	GAGE 3 (G's)
1	1	16.6	>4.7	0.091	-	-	-	-	-	-
2	1	16.6	7.3	0.087	156	154	-	17	11	-
3	1	2.4	6.4	0.495	133	154	154	15	-	-
4	1	0	6.3	2.000	125	167	167	13	-	-
5	2	16.6	14.6	0.136	167	182	-	17	20	-
6	2	2.4	12.9	0.680	182	167	167	30	-	-
7	2	0	12.9	2.670 [2]	200	176	176	25	-	-
8	5	16.6	31.3	0.167	182	133	-	81	68	-
9	5	16.6	31.3	0.162	172	182	172	69	64	63
10	5 [3]	16.6	33.0	0.167	200	172	172	88	-	-
11	5	2.4	31.4	1.100 [2]	172	172	172	78	-	-
12	5	1.2 [4]	27.8	3.200	182	172	172	87	-	-
13	5	0	32.6	3.500 [2]	182 [5]	-	-	63	-	-

NOTES:
1. DOOR COMPLETELY OPEN FOR VENT AREA OF 16.6 FT^2; COMPLETELY CLOSED FOR 0 FT^2.
2. THESE ARE ESTIMATED VALUES.
3. NEIGHBOR COMPLAINED ON THIS TEST FIRING.
4. VENT AREA UNCERTAIN BECAUSE OF DOOR DAMAGE.
5. WALL VIBRATION WAS COMPLETED IN ABOUT 150 MSEC.

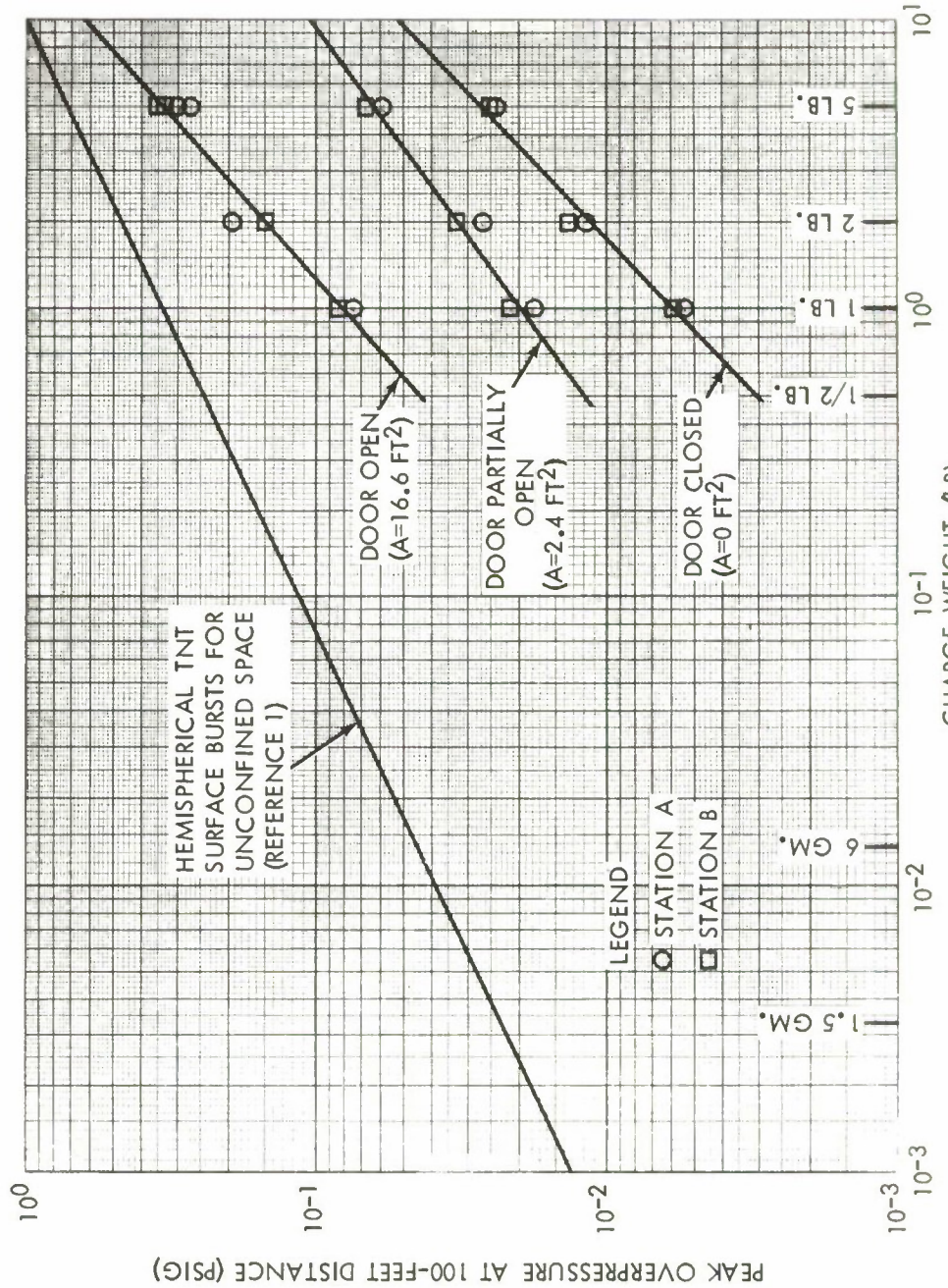

FIG. 4 OUTSIDE PRESSURE VS CHARGE WEIGHT FOR VARIOUS VENT AREAS

Internal Shock Loading. No attempt was made to obtain experimental data on the internal shock loading of the bombproof walls. Because of the multiple reflected shocks from adjacent walls, an experimental effort to define adequately the shock loadings on one wall would require a large number of face-on piezoelectric pressure gages. Such an expensive undertaking was not within the scope of this task. However, Picatinny Arsenal has been studying the shock loading on and response of concrete walls to close-in explosions for various degrees of building enclosures. In reference (2) a series of curves based on experimental and analytical data are presented that define an upperbound average impulse on a chamber wall from large close-in explosions. From Figures 4-15 and 4-61 of reference (2), it can be shown that the longest wall span (21 ft) in Building 324 receives an average 25.4-psf-sec impulsive load from the detonation of a 5-lb TNT charge. The degree of conservatism in this impulse value cannot be defined. Reference (3), an earlier publication by Picatinny Arsenal on this work, indicated that, for similar building configurations and equal charge weights, the ratio of calculated impulse to experimentally measured impulse increased as the distance from the charge to the wall was increased. From presented data, it showed that for charges of 1.4 and 2.6 lb with distances from 5.5 to 16.5 inches, the ratio could increase 20 to 30 percent. Since our 5-lb explosion in the bombproof just falls within the limits of the empirical curves of reference (2), the degree of conservatism could be at least 20 percent and possibly could be much higher.

Internal Gas Pressure. From reference (4) the equilibrium gas overpressure for an enclosed explosion is given by the expression

$$P = 4000\ hW/V_o$$

where P .... overpressure psig
h .... heat of combustion of explosive, kcal/gm
W .... weight of explosive, lb
V_o .... volume of chamber, ft^3

The enclosed volume of Building 324 is 2,010 ft^3. For pentolite with h = 2.76 kcal/gm (reference (4)), the above relation becomes

$$P = 5.49\ W_{(pentolite)} \qquad (1)$$

Reference (2) gives the gas overpressure for TNT charges by the empirical equation

$$P = 2410\ (W/V_o)^{0.72}$$

The equivalent weight table in reference (4) gives

$$W_{TNT} = 1.17\ W_{pentolite}$$

Thus the equation for gas overpressure becomes for pentolite and a chamber volume of 2,010 ft^3

$$P = 11.2\ (W_{pentolite})^{0.72} \qquad (2)$$

For the particular tests conducted in Building 324, the following table compares calculated gas overpressures from Equations (1) and (2) with the average experimental values from Table 2.

W (lb)	Calculated Overpressure (psig) Eq. 1	Eq. 2	Average Experimental Overpressure (psig)
1	5.5	11.2	6.7
2	11.0	18.4	13.5
5	27.5	35.6	31.2

The reason for the wide span between the calculated pressures, particularly for the smaller charge weights, is not known and will not be pursued here. It is noted that the experimental results fall close to the pressures calculated by reference (4) methods, but they are some 15 to 20 percent higher.

Venting of Internal Gas Pressure. An important parameter in structural response considerations is the duration of this gas pressure. Although the vent times were experimentally recorded for the subject tests, it is desirable to devise an analytical technique for estimating the venting process and to compare the two sets of results. Let us denote the equilibrium gas pressure defined in the previous section by P_o where now this pressure is expressed in absolute terms -- psia. We assume P_o is fully developed before any venting occurs. The vent area is denoted by A. Further we assume at the beginning of the expansion that P_o is sufficiently large to ensure sonic flow through the vent area A, i.e., perfect isentropic nozzle flow through A. This should result in the calculation of minimum vent times. Thus

$$P_o \geq P_c \tag{3}$$

where P_c is the critical throat pressure associated with sonic throat velocity and is defined in any thermodynamics text as

$$P_c = \frac{P_a}{\left(\frac{2}{\gamma+1}\right)^{\frac{\gamma}{\gamma-1}}} \tag{4}$$

where P_a is the exhaust pressure which in our case is atmospheric pressure (14.696 psia), and γ is the conventional ratio of specific heats.

The mass flow through area A is given as

$$- dM = \rho_e v_e A \, dt \tag{5}$$

where M .... mass of gas
ρ .... density of gas
v .... velocity of gas
t .... time

and the subscript e denotes conditions at the nozzle throat A. Letting the subscript o denote initial conditions in the chamber and the subscript 1 denote conditions in the chamber at any instant of time, we can write

$$M = \rho_1 V_o \qquad \text{and} \qquad dM = V_o \, d\rho_1 \tag{6}$$

Then (5) and (6) become

$$- V_o \, d\rho_1 = \rho_e v_e A \, dt \tag{7}$$

The isentropic expansion process allows us to relate the instantaneous pressure and density to the initial conditions by

$$P_1/\rho_1{}^{\gamma} = P_o/\rho_o{}^{\gamma} \tag{8}$$

from which one derives

$$d\rho_1 = \frac{1}{\gamma} (\rho_o{}^{\gamma}/P_o)^{1/\gamma} \frac{dP_1}{P_1^{\frac{\gamma-1}{\gamma}}} \tag{9}$$

Then a combination of (7) and (9) results in

$$- \frac{dP_1}{P_1^{\frac{\gamma-1}{\gamma}}} = \gamma (P_o/\rho_o{}^{\gamma})^{1/\gamma} \rho_e v_e \frac{A}{V_o} dt \tag{10}$$

Since the flow is sonic at the throat

$$\rho_e v_e = (\gamma \rho_e P_e)^{1/2}, \tag{11}$$

$$P_e/P_1 = \left(\frac{2}{\gamma+1}\right)^{\frac{\gamma}{\gamma-1}}, \tag{12}$$

and for the isentropic expansion

$$\rho_e = \rho_1 (P_e/P_1)^{1/\gamma} \tag{13}$$

Substituting (12) and (13) into (11), we obtain

$$\rho_e v_e = \left[\gamma \left(\frac{2}{\gamma+1}\right)^{\frac{\gamma+1}{\gamma-1}} (\rho_o{}^{\gamma}/P_o)^{1/\gamma} P_1^{\frac{\gamma+1}{\gamma}}\right]^{1/2} \tag{14}$$

A combination of (10) and (14) in integration form with appropriate limits becomes

$$- \int_{P_o}^{P_1} \frac{dP_1}{P_1^{\frac{3\gamma-1}{2\gamma}}} = \left[\gamma^3 (P_o{}^{1/\gamma}/\rho_o)\left(\frac{2}{\gamma-1}\right)^{\frac{\gamma+1}{\gamma-1}}\right]^{1/2} \frac{A}{V_o} \int_o^t dt \tag{15}$$

Integrating (15) remembering that P_1 is instantaneous pressure and at $t = 0$, $P_1 = P_o$, we find

$$P_1 = P_o \left[1 + \left(\frac{\gamma-1}{2}\right)\left(\frac{2}{\gamma+1}\right)^{\frac{\gamma+1}{2(\gamma-1)}} \left(\frac{\gamma P_o}{\rho_o}\right)^{1/2} \frac{A}{V_o} t\right]^{-\frac{2\gamma}{\gamma-1}} \tag{16}$$

This equation is valid only when

$$P_o \geq P_1 \geq P_c = \frac{P_a}{\left(\frac{2}{\gamma+1}\right)^{\frac{\gamma}{\gamma-1}}} = \frac{14.696}{\left(\frac{2}{\gamma+1}\right)^{\frac{\gamma}{\gamma-1}}} \tag{17}$$

When (17) is violated, i.e., when the flow becomes subsonic, the velocity in the throat is the same as the discharge velocity which is given by

$$v_e = v_a = \left(\frac{2}{\gamma-1}\right)^{1/2} \left(\frac{\gamma P_1}{\rho_1}\right)^{1/2} \left[1 - \left(\frac{P_a}{P_1}\right)^{\frac{\gamma-1}{\gamma}}\right]^{1/2} \tag{18}$$

Also

$$\rho_e v_e = \rho_a v_a \tag{19}$$

The flow process across the nozzle and the chamber expansion remain isentropic, thus

$$\rho_a = (P_a/P_1)^{1/\gamma} \rho_1 \tag{20}$$

$$\rho_1 = (P_1/P_o)^{1/\gamma} \rho_o \tag{21}$$

With (18), (20), and (21), (19) can be written as

$$\rho_e v_e = \left(\frac{2}{\gamma-1}\right)^{1/2} \left[\gamma \rho_o (P_1/P_o)^{1/\gamma} P_1\right]^{1/2} (P_a/P_1)^{1/\gamma} \left[1 - (P_a/P_1)^{\frac{\gamma-1}{\gamma}}\right]^{1/2} \tag{22}$$

Substituting (22) into (10), we obtain

$$-\frac{P_1^{-\frac{\gamma-1}{\gamma}} dP_1}{\left(P_1^{\frac{\gamma-1}{\gamma}} - P_a^{\frac{\gamma-1}{\gamma}}\right)^{1/2}} = \left[\gamma^3 \left(\frac{2}{\gamma-1}\right)\left(\frac{P_o P_a^2}{\rho_o \gamma}\right)^{1/\gamma}\right]^{1/2} \frac{A}{V_o} dt \tag{23}$$

Let

$$n = (\gamma - 1)/\gamma \tag{24}$$

With appropriate integration limits, (23) becomes

$$\int_{P_c}^{P_1} \frac{P_1^{-n}\, dP_1}{(P_1^n - P_a^n)^{1/2}} = -\left[\gamma^3 \left(\frac{2}{\gamma-1}\right)\left(\frac{P_o\, P_a^{\,2}}{\rho_o^{\,\gamma}}\right)^{1/\gamma}\right]^{1/2} \frac{A}{V_o} \int_{t_c}^{t} dt \qquad (25)$$

The problem now is to evaluate the integral on the left-hand side of (25). We start by letting

$$P_1^n - P_a^n = x^2 \qquad (26)$$

It follows that

$$dP_1 = \frac{2x\, dx}{n\, P_1^{n-1}}$$

Then the left-hand side of (25) can be written as

$$\int \frac{P_1^{-n}\, dP_1}{(P_1^n - P_a^n)^{1/2}} = 2/n \int P_1^{-(2n-1)}\, dx \qquad (27)$$

From (26), we can determine

$$P_1^{-(2n-1)} = (x^2 + P_a^n)^{\frac{-(2n-1)}{n}}$$

For air $\gamma = 1.4$, thus $n = 2/7$ and $-(2n - 1)/n = 3/2$. Letting $P_a^n = C^2$(constant), we can now write (27) as

$$\int \frac{P_1^{-n}\, dP_1}{(P_1^n - P_a^n)^{1/2}} = 2/n \int (x^2 + C^2)^{3/2}\, dx$$

From Case 139 of reference (5), this integral is given as

$$\int (x^2 + C^2)^{3/2}\, dx = \frac{1}{4}\left\{x(x^2 + C^2)^{3/2} + \frac{3C^2x}{2}(x^2 + C^2)^{\frac{1}{2}} + \frac{3C^4}{2} \ln\left[x + (x^2 + C^2)^{\frac{1}{2}}\right]\right\}$$

Using this integration technique, we can evaluate (25) as

$$P_1^{n/2}(P_1^n - P_a^n)^{1/2}(P_1^n + 3/2\,P_a^n) + \tfrac{3}{2}P_a^{2n}\ln\left[P_1^{n/2} + (P_1^n - P_a^n)^{\frac{1}{2}}\right]$$

$$-P_c^{n/2}(P_c^n - P_a^n)^{1/2}(P_c^n + 3/2\,P_a^n) - \tfrac{3}{2}P_a^{2n}\ln\left[P_c^{n/2} + (P_c^n - P_a^n)^{\frac{1}{2}}\right]$$

$$= -2n\left[\gamma^3\left(\frac{2}{\gamma-1}\right)\left(\frac{P_o P_a^2}{\rho_o \gamma}\right)^{1/\gamma}\right]^{1/2}\frac{A}{V_o}(t - t_c) \qquad (28)$$

where again $n = (\gamma - 1)/\gamma$ and t_c is the time corresponding to P_c as determined from (16).

In review, assume that $P_o \geq P_c$, then (16) describes the pressure-time decay until $P_1 = P_c$ at time $t = t_c$. Then the decay is described by (28) until $P_1 = P_a$ at which time the chamber pressure equals atmospheric pressure and venting is complete. Now, if initially $P_o < P_c$, (16) cannot be used, and only (28) describes the decay function. In this case P_c should be set equal to P_o and t_c set equal to zero in (28).

From the above derived equations, the analytical estimates for vent times can be compared with the experimental values as is shown in Figure 5. For the 16.6-ft^2 vent area (door fully open) we note that the calculated curve does indeed represent minimum vent times. The difference for the most part is believed attributable to the imperfect nozzle flow through the vent area and the effects of high-speed diffraction around the labyrinth corners. At the 2.4-ft^2 vent area (door partially open) the predicted curve is still basically below the experimental curve, but they are much closer together. Here it is believed that the imperfect flow effects are being offset by heat losses occurring in the chamber due to the longer total duration times. The uppermost curve is that obtained experimentally for the completely-closed door condition. Here heat losses and gas leakage losses have combined to produce this finite limit curve.

From Figure 5 it is seen that the total duration for a 5-lb explosion varies from about 160 milliseconds for the door fully open to about 3.5 seconds for the door completely closed -- over an order of magnitude difference. From this one could hastily conclude that the loading for the closed-door condition should result in much greater wall stresses and deflections than that from the open-door

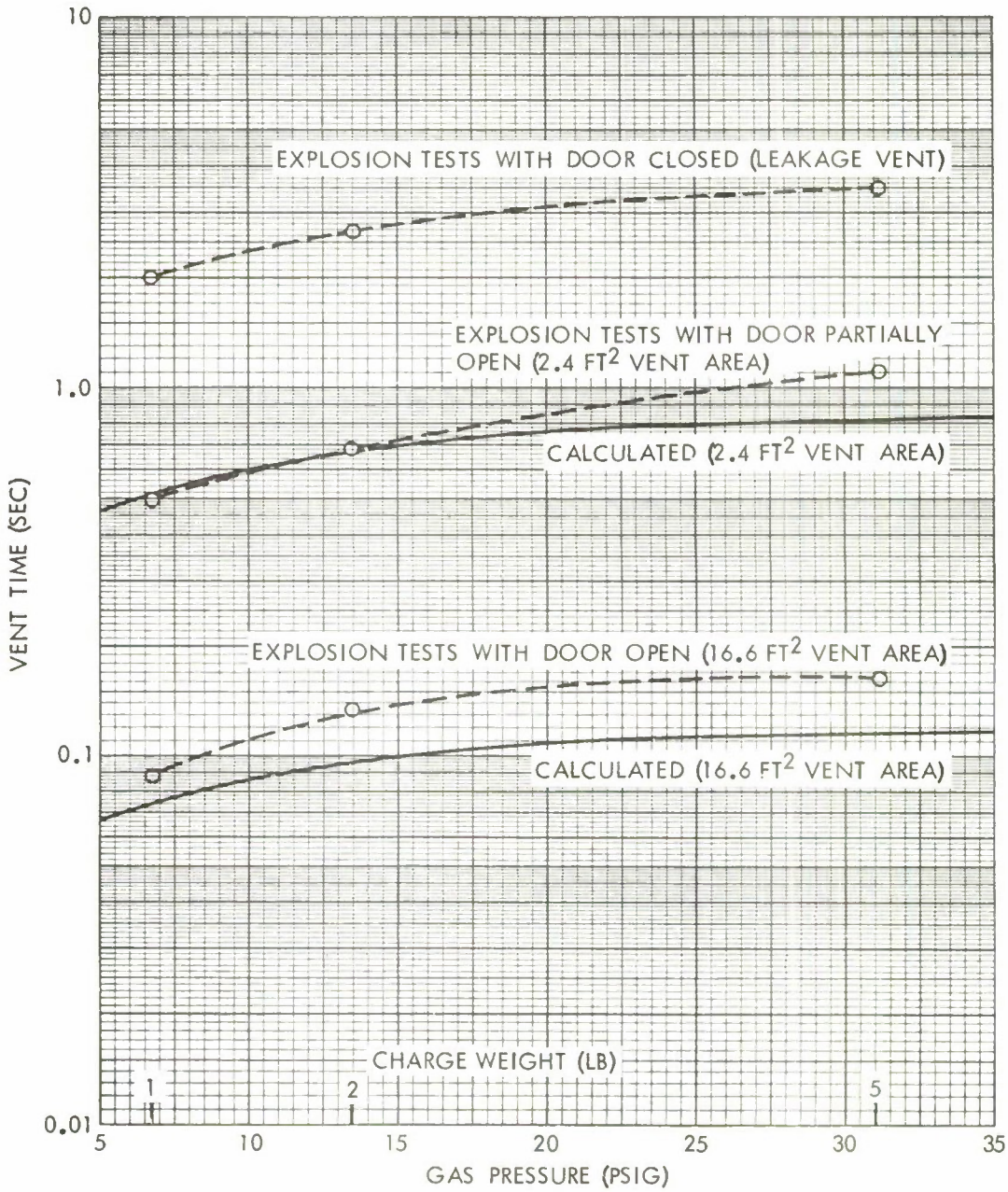

FIG. 5 COMPARISON OF CALCULATED AND EXPERIMENTAL VENT TIMES

loading. However, this is not true. Figure 6 gives a calculated approximation of the gas pressure-time decay curve derived from Equations (16) and (28) for a 5-lb explosion with the maximum vent area of 16.6 ft^2. In the next section of the report it is shown that the natural frequency of the slowest responding wall is about 174 Hz, or the wall has a natural period of 5.7 milliseconds or a quarter natural period of about 1.4 milliseconds. Since the maximum wall deflection should theoretically occur at the 1.4-msec time, we see from Figure 6 that the pressure has dropped less than 3 percent for this the fastest decaying situation. Essentially, then, the wall views this most rapid decay as a quasi-static, constant uniform load - the same as it views the longer duration vent times. Therefore, it is extremely doubtful that the door condition for these bombproofs has any significant effect on the maximum wall stress level or deflection.

Wall Response Measurements. Table 2 gives the natural frequencies and peak accelerations taken from the three accelerometers mounted at the center of the longest wall (see Figure 1). From the data on the 5-lb explosion, the following observations were made:

Natural Frequency, f (Hz)

Low	Average	High
133	174	200

Natural Period, T (msec)

Low	Average	High
5.0	5.7	7.5

Natural Quarter Period, T/4 (msec)

Low	Average	High
1.3	1.4	1.9

Peak Acceleration, a_p (g's)

Low	Average	High
63	73	88

If we assume that the center of the wall undergoes deflections characterized by simple harmonic motion, then the maximum deflection y_p (inches) is related to the peak acceleration a_p (g's) by the relation

$$y_p = \frac{(32.2)(12)\, a_p}{(2\pi)^2 f^2} = 9.79\, a_p/f^2$$

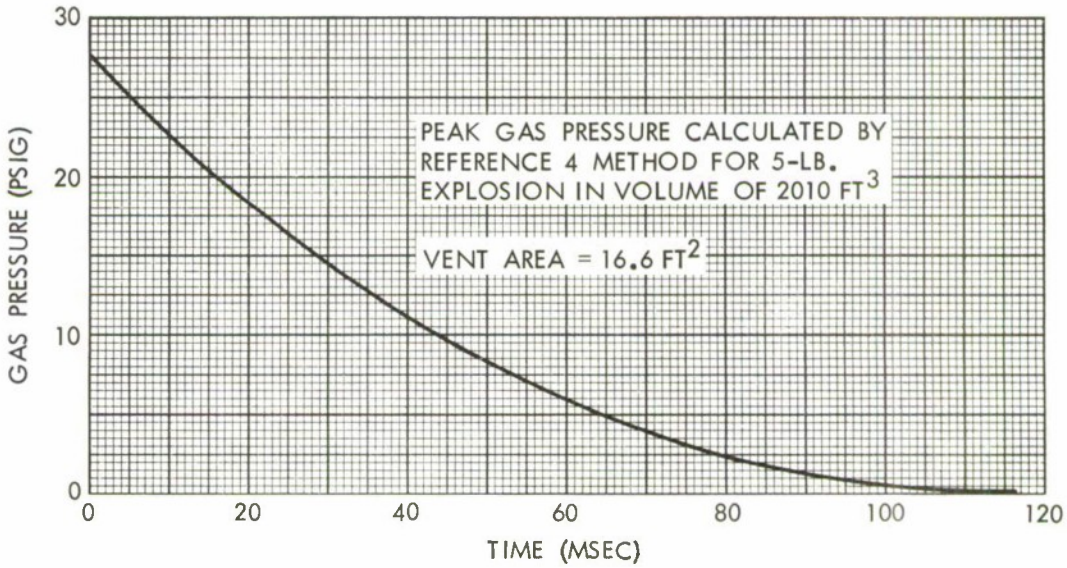

FIG. 6 GAS PRESSURE DECAY FOR CASE OF OPEN DOOR

For the above range of frequencies and peak accelerations, the maximum wall deflection for the 5-lb explosion falls within the band shown in Figure 7. The single dot within the band represents the deflection corresponding to the average frequency and average acceleration.

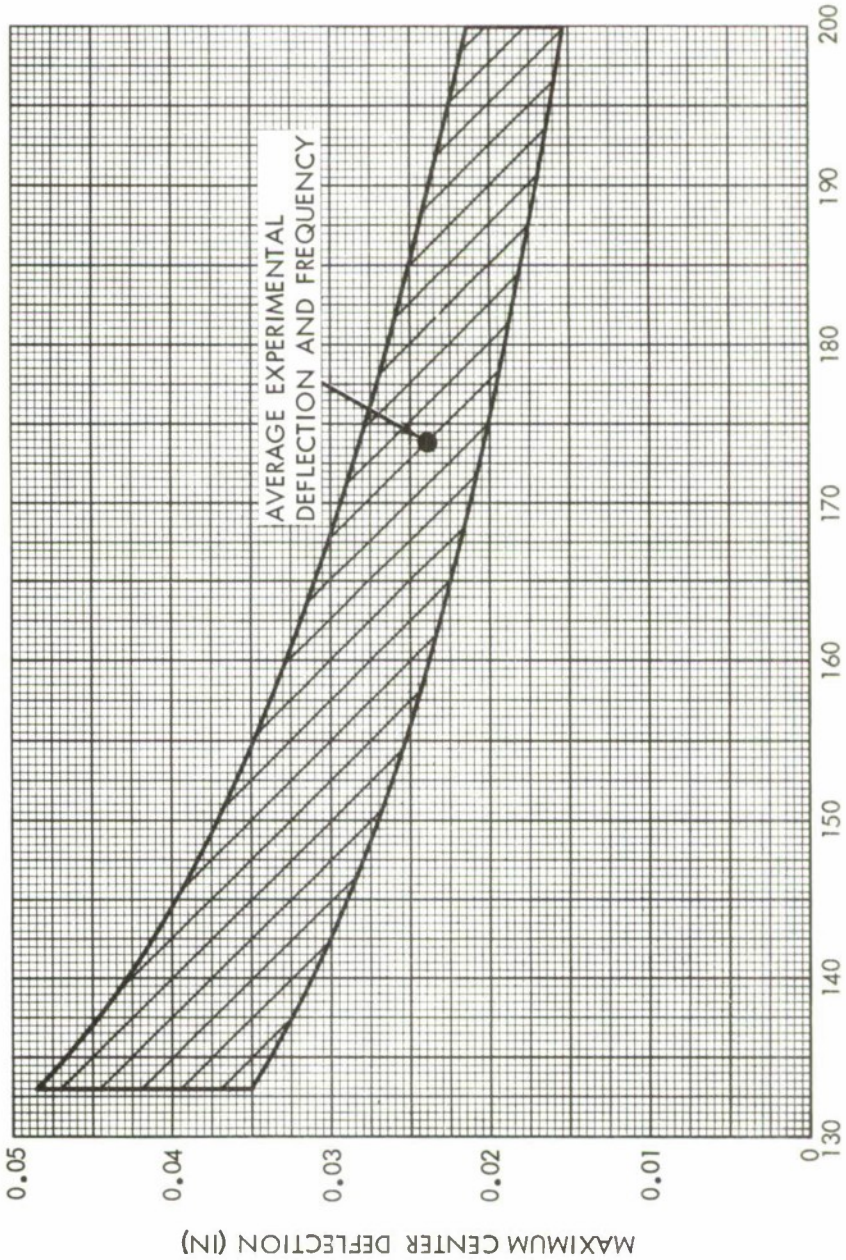

FIG. 7 EXPERIMENTAL WALL RESPONSE BAND

STRUCTURAL ANALYSIS

Classification of Wall. From a preliminary observation of the construction of the 8.5-ft high by 21-ft wide (weakest) wall of the bombproof, one would speculate that (1) the wall could be considered a wide (plane strain) beam because of its large width to height ratio and that (2) the edges could be considered fixed because of the heavy corner reinforcement (see Figure 2). To analyze the soundness of the first assumption, we compare the equations of center deflection, maximum stress, and natural frequency for a fixed-edge plate of width-to-height ratio of $h/\ell = 21/8.5 = 2.47$ and a wide (plane strain) fixed-end beam, both with a uniform load of pressure P. (t denotes wall thickness in below equations.)

Fixed Plate (h/ℓ=2.47)	Fixed Beam (wide)	Difference
	Center Deflection (reference (6))	
$y_c = 0.0280\ P\ell^4/Et^3$	$y_c = 0.0284\ P\ell^4/Et^3$	1%
	Maximum Stress (reference (6))	
$\sigma_{max} = 0.5\ P\ell^2/t^2$	$\sigma_{max} = 0.5\ P\ell^2/t^2$	0%
	Natural Frequency (references (7) and (8))	
$f = \frac{12}{\pi\ell^2}\sqrt{\frac{12\ Et^2g}{(1-\nu^2)\rho}}$	$f = \frac{11.2}{\pi\ell^2}\sqrt{\frac{12\ Et^2g}{(1-\nu^2)\rho}}$	7%

We conclude from the above comparison based on standard references that the wall can be considered a wide beam with little loss in accuracy.

To assess the validity of the second assumption, we compare the frequency equations for a fixed-end beam and a simply-supported beam.

Fixed End	Simply Supported
$f = \frac{11.2}{\pi\ell^2}\sqrt{\frac{12\ Et^2g}{(1-\nu^2)\rho}}$	$f = \frac{4.93}{\pi\ell^2}\sqrt{\frac{12\ Et^2g}{(1-\nu^2)\rho}}$

It is difficult to define the effective length ℓ of our beam, but it certainly must fall in the range of 8.5 ft to 12.5 ft (2-ft roof and floor thicknesses). Using these two extremes we find that the frequency of the fixed-end beam falls between 290 and 134 Hz and the frequency of the simply-supported beam ranges between 128 and 59 Hz for the conditions

$E = 3.149 \times 10^6$ psi (concrete - reference (9))

$\rho = 145$ lb/ft^3 (concrete - reference (9))

$\nu = 0.17$ (concrete - reference (9))

$t = 2$ ft

$g = 32.2$ ft/sec^2

Since the measured wall frequencies ranged between 133 and 200 Hz (average 174 Hz -- see Figure 7), we conclude that a fixed-end beam is a reasonable assumption.

Stresses in Wall. As shown in the previous section, the effective length of the fixed-end beam that represents the bombproof long wall is greater than the 8.5-ft interior height. We find from the frequency equation

$$f = \frac{11.2}{\pi \ell^2} \sqrt{\frac{12\, Et^2 g}{(1-\nu^2)\rho}} \tag{29}$$

that, for the extreme measured frequencies of 133 and 200 Hz, the effective lengths ℓ are 12.55 and 10.24 ft, respectively. For the average frequency 174 Hz, $\ell = 10.98$ ft. It seems prudent here to examine the response of these three beams to form a family of response curves.

The subject beam is loaded only over the 8.5-ft internal height. Therefore the case of a fixed-end beam with a partial uniform load (symmetric about the center of the beam) depicted in Figure 8 best represents our beam. Referring to Case 34 of Table III in reference (6), the equations for reaction forces, moments, and deflections are given below for a wide beam of rectangular cross-section.

$$R_1 = R_2 = Pb/2 \tag{30}$$

$$M_1 = M_2 = \frac{Pb}{24\ell}(3\ell^2 - b^2) \tag{31}$$

$$\text{from (A to B)} \quad M = -M_1 + R_1 x \tag{32}$$

$$\text{from (B to D)} \quad M = -M_1 + R_1 x - \tfrac{1}{2}Pb\,(x - a)^2/b \tag{33}$$

$$\text{from (A to B)} \quad y = \frac{2(1-\nu^2)}{Et^3}(R_1 x^3 - 3M_1 x^2) \tag{34}$$

$$\text{from (B to C)} \quad y = \frac{2(1-\nu^2)}{Et^3}\left[R_1 x^3 - 3M_1 x^2 - \tfrac{1}{4}P\,(x - a)^4\right] \tag{35}$$

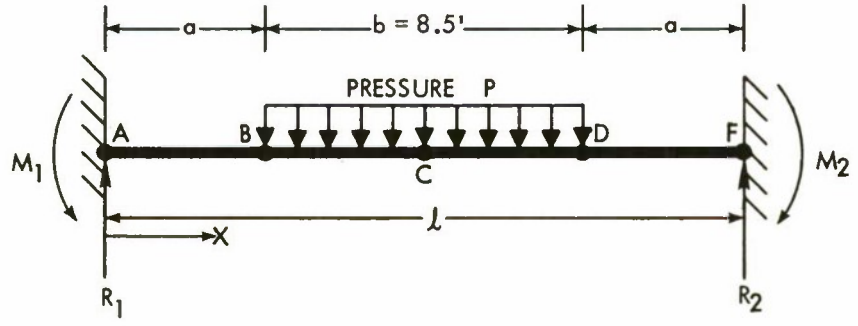

FIG. 8 FIXED-END BEAM WITH PARTIAL UNIFORM LOAD

where R_1, R_2 .... reaction forces at ends
M_1, M_2 .... moments at ends
M .... bending moment at any point on beam
y .... deflection at any point on beam
x .... coordinate along length
P .... uniform pressure
t .... thickness of beam
E .... modulus of elasticity of concrete
ν .... Poisson's ratio of concrete
b .... length of beam on which P acts
a .... unloaded portion of beam

The moment distribution within the junction of two walls falls outside the scope of this elementary analysis. Therefore only moments and deflections will be examined where actual cracks in the concrete walls have been observed; namely, at the center (point C) and at the corner (point B). At the center (point C) $x = \ell/2$, the moment and deflection from Equations (33) and (35) become

$$M_c = \frac{Pb}{4}\left[-\frac{(3\ell^2 - b^2)}{6\ell} + \ell - b/2\right] \tag{36}$$

$$y_c = \frac{Pb\,(1-\nu^2)}{8\,Et^3}\left[\ell^3 - \frac{(3\ell^2 - b^2)\ell}{2} - b^3/4\right] \tag{37}$$

At the corner (point B) $x = a = (\ell-b)/2$, the moment and deflection from Equations (32) and (34) become

$$M_B = \frac{Pb}{4}\left[-\frac{(3\ell^2 - b^2)}{6\ell} + \ell - b\right] \tag{38}$$

$$y_B = \frac{Pb\,(1-\nu^2)(\ell-b)^2}{8\,Et^3}\left[(\ell-b) - \frac{(3\ell^2 - b^2)}{2\ell}\right] \tag{39}$$

It is now possible to write M_c, M_B, and y_B in terms of y_c by eliminating the pressure term P. For the 2-ft concrete walls, t = 2 ft, $E = 3.149 \times 10^6$ psi, $\nu = 0.17$, and the correct units

$$M_c = (6.228 \times 10^6)\, y_c \frac{\left[-\frac{(3\ell^2 - b^2)}{6\ell} + \ell - b/2\right]}{\left[\ell^3 - \frac{(3\ell^2 - b^2)\ell}{2} - b^3/4\right]} \text{ (lb-in/in)} \tag{40}$$

$$M_B = (6.228 \times 10^6)\, y_c \frac{\left[-\frac{(3\ell^2 - b^2)}{6\ell} + \ell - b\right]}{\left[\ell^3 - \frac{(3\ell^2 - b^2)\ell}{2} - b^3/4\right]} \text{ (lb-in/in)} \tag{41}$$

$$y_B = y_c\,(\ell - b)^2 \frac{\left[(\ell - b) - \frac{(3\ell^2 - b^2)}{2\ell}\right]}{\left[\ell^3 - \frac{(3\ell^2 - b^2)\ell}{2} - b^3/4\right]} \text{ (in)} \tag{42}$$

Failure or cracking of the concrete wall will begin when the tensile stress in the reinforcing steel exceeds its elastic limit. Therefore the reinforcing steel on the compression side of the wall can be neglected with little loss in accuracy. For the straight-line theory analysis, references (10) and (11), the governing equations are

$$k = n\sigma_c/(\sigma_s + n\sigma_c) \tag{43}$$

$$j = 1 - k/3 \tag{44}$$

$$M = A_s\, \sigma_s\, j\, d \tag{45}$$

$$\sigma_c = 2M/jkd^2 \tag{46}$$

where A_s .... cross-sectional area of tensile reinforcing steel per unit width of beam, in^2/in

d .... distance from extreme compression fibers to center of tensile reinforcing steel, in

k, j .... ratios as defined by (43) and (44)

M .... bending moment in beam, lb-in/in

n .... ratio of modulus of elasticity of steel to that of concrete

σ_s .... stress in steel, psi

σ_c .... stress in concrete, psi

For our particular wall

$$d = 21 \text{ in}$$
$$n = (29 \times 10^6)/(3.149 \times 10^6) = 9.21$$
$$A_s = (0.75)^2/32 = 0.0552 \text{ in}^2/\text{in}$$

A rearrangement of (43) yields

$$\left(1 + \frac{\sigma_s}{n\sigma_c}\right) k - 1 = 0 \tag{47}$$

Combining (45) and (46) we find

$$\frac{\sigma_s}{n\sigma_c} = \frac{kd}{2n\,A_s} \tag{48}$$

Substituting (48) into (47) we obtain

$$\left(1 + \frac{kd}{2n\,A_s}\right) k - 1 = 0$$

or

$$k^2 + \frac{2n\,A_s}{d}\,k - \frac{2n\,A_s}{d} = 0 \tag{49}$$

The solution of (49) for k is

$$k = -\frac{nA_s}{d} + \sqrt{\frac{nA_s}{d}\left(\frac{nA_s}{d} + 2\right)}$$

For the previously given values of n, d, and A_s,

$$k = 0.1972 ,$$

from (44)

$$j = 0.9343 ,$$

and from (45)

$$\sigma_s = 0.9233\ M \tag{50}$$

Therefore (50) in combination with (40) and (41) will yield the stresses at the beam center and corner as functions of the center deflection. Table 3 and Figure 9 show these functional relationships. From Table 3 we note that the tensile stress

TABLE 3 - BEAM STRESSES AND DEFLECTIONS

FREQUENCY (Hz)	EFFECTIVE LENGTH (FT)	CENTER DEFLECTION (IN)	CORNER DEFLECTION (IN)	STRESS AT CENTER (PSI)	STRESS AT CORNER (PSI)
133	12.55	0.01	0.0028	24,900	10,600
		0.02	0.0057	49,800	21,200
		0.03	0.0085	74,700	31,800
		0.04	0.0113	99,600	42,400
		0.05	0.0142	124,500	53,000
174	10.98	0.01	0.0016	32,100	26,200
		0.02	0.0031	64,200	52,400
		0.03	0.0047	96,300	78,600
		0.04	0.0063	128,400	104,800
		0.05	0.0079	160,500	131,000
200	10.24	0.01	0.0010	36,800	39,400
		0.02	0.0019	73,600	78,800
		0.03	0.0029	110,400	118,200
		0.04	0.0038	147,200	157,600
		0.05	0.0048	184,000	197,000

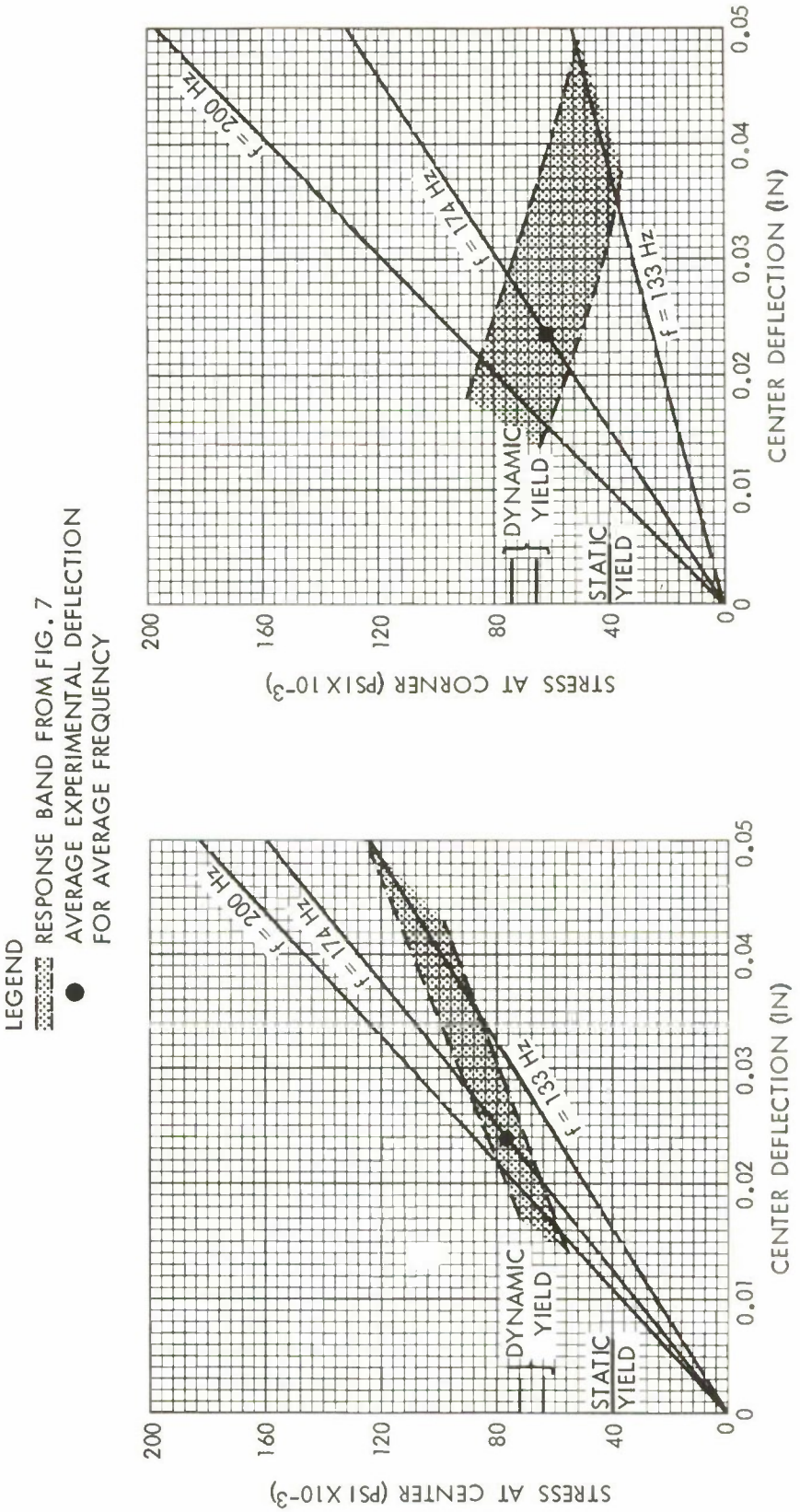

FIG. 9 COMPARISON OF CALCULATED AND EXPERIMENTALLY-DERIVED WALL STRESSES

at the center and corner for the average 174-Hz frequency and 200-Hz upper-limit frequency are nearly equal -- somewhere between these two they would be exactly equal. Also for these two frequencies it is noted that the deflection at the corner is very small -- an order of magnitude lower than the center deflection.

Superposed on the curves in Figure 9 is the experimentally obtained response band (shaded area) for a 5-lb explosion from Figure 7, and the large dot represents the average frequency and center deflection. It can be shown that the maximum strain rate in the steel reinforcing is about 1.5 sec^{-1} for this frequency range. From reference (12) the dynamic yield stress for mild steel at this strain rate is between 1.6 to 1.8 times greater than the static yield stress. Therefore for a 40,000-psi static yield, the dynamic yield stress ranges between 64,000 and 72,000 psi. These levels of stress are indicated on the curves in Figure 9. We note that the major portion of the shaded band falls above the dynamic yield stress level for the mid-height wall stress, whereas the major portion of the band falls below the dynamic yield stress for the corner stress. This observation indicates that the 5-lb explosion does produce stresses that slightly exceed the yield capacity of the wall and explains why more and larger cracks are observed at the wall mid-height than at the inside corners.

Predictions Based on Impulse. In the previous section we have examined wall stresses derived from experimental acceleration data for a 5-lb explosion. The question is -- how well could we have predicted this response? In the section "Experimental and Analytical Results - Internal Shock Loading," it was estimated that the wall was given an impulse of 25.4 psf-sec for a 5-lb explosion. However, it was pointed out that this impulse could be conservative by at least 20 percent if not much greater. Using the simplest approach, we assume that this impulse gives the wall an instantaneous velocity or kinetic energy as described by the equation

$$KE = I^2/2M$$

where KE .... kinetic energy, ft-lb
I .... impulse, lb-sec/ft^2
M .... mass, slugs/ft^2

From the construction details shown in Figure 2, the wall mass per square-foot area can be found to be 10.8 slugs/ft^2 (this includes mass of concrete, reinforcing steel on both sides, wood liner, and armor plate). Then

$$KE = I^2/(2)(10.8) = 0.0463\ I^2 \quad (ft\text{-}lb/ft^2)$$

If we wish to express the kinetic energy on a unit beam-width basis, we need to multiply the above by the loaded wall height (8.5 ft)

$$KE = 0.394\ I^2 \quad (ft\text{-}lb/ft) \tag{51}$$

Our approach now is to express the strain energy of the beam in terms of center deflection, equate this energy to the initial kinetic energy (51), and solve for the center deflection. For the case of a fixed-end wide beam with a partial uniform load (see Figure 8), the strain energy SE per unit width of beam is defined as

$$SE = \int_o^y \int_a^d P\ dx\ dy\ ;\ d = a + b \tag{52}$$

Combining Equation (35) with (30) and (31), we can express the deflection of the beam in the region of a to d (from B to C) as

$$y = \frac{(1-\nu^2)Pb}{Et^3}\left[x^3 - \frac{(3\ell^2 - b^2)x^2}{4\ell} - \frac{(x-a)^4}{2b}\right] \tag{53}$$

Also

$$dy = \frac{(1-\nu^2)b}{Et^3}\left[x^3 - \frac{(3\ell^2 - b^2)x^2}{4\ell} - \frac{(x-a)^4}{2b}\right] dP \tag{54}$$

Substituting (54) into (52) and changing limits, we obtain

$$SE = \frac{(1-\nu^2)b}{Et^3} \int_o^P \int_a^d P\left[x^3 - \frac{(3\ell^2-b^2)x^2}{4\ell} - \frac{(x-a)^4}{2b}\right] dx\ dp \tag{55}$$

Integrating (55) yields

$$SE = \frac{(1-\nu^2)\,P^2 b}{4\,Et^3}\left[\frac{(d^4-a^4)}{2} - \frac{(3\ell^2-b^2)(d^3-a^3)}{6\ell} - \frac{(d-a)^5}{5b}\right] \tag{56}$$

From the geometry of the problem

$$a = (\ell-b)/2 \qquad \text{and} \qquad d = a+b = (\ell+b)/2$$

and the substitution of these into (56) produces

$$SE = \frac{(1-\nu^2)\,P^2 b^2}{4\,Et^3}\left[\frac{\ell(\ell^2+b^2)}{4} - \frac{(9\ell^4-b^4)}{24\ell} - b^3/5\right] \tag{57}$$

To eliminate P from (57), we substitute (37) which gives

$$SE = y_c^2 \cdot \frac{16\,Et^3}{(1-\nu^2)} \frac{\left[\frac{\ell(\ell^2+b^2)}{4} - \frac{(9\ell^4-b^4)}{24\ell} - b^3/5\right]}{\left[\ell^3 - \frac{(3\ell^2-b^2)\ell}{2} - b^3/4\right]^2} \tag{58}$$

where ℓ, b, t ... ft; E ... lb/in^2; y_c ... in; and SE ... ft-lb/ft.

We see in (58) that the beam strain energy is expressed as a function of the center deflection. A combination of (51) and (58) yields

$$y_c = (3.081 \times 10^{-5})\, I \frac{\left[\ell^3 - \frac{(3\ell^2-b^2)\ell}{2} - b^3/4\right]}{\left[\frac{\ell(\ell^2+b^2)}{4} - \frac{(9\ell^4-b^4)}{24\ell} - b^3/5\right]^{\frac{1}{2}}} \tag{59}$$

Since the degree of conservatism associated with the predicted impulse I_i = 25.4 psf-sec is in doubt, we elect to examine the predicted deflections for I_i and $I_i/2$. The resultant two curves (dashed) for the frequency range of interest are shown in Figure 10. Also shown in this figure is the experimental response

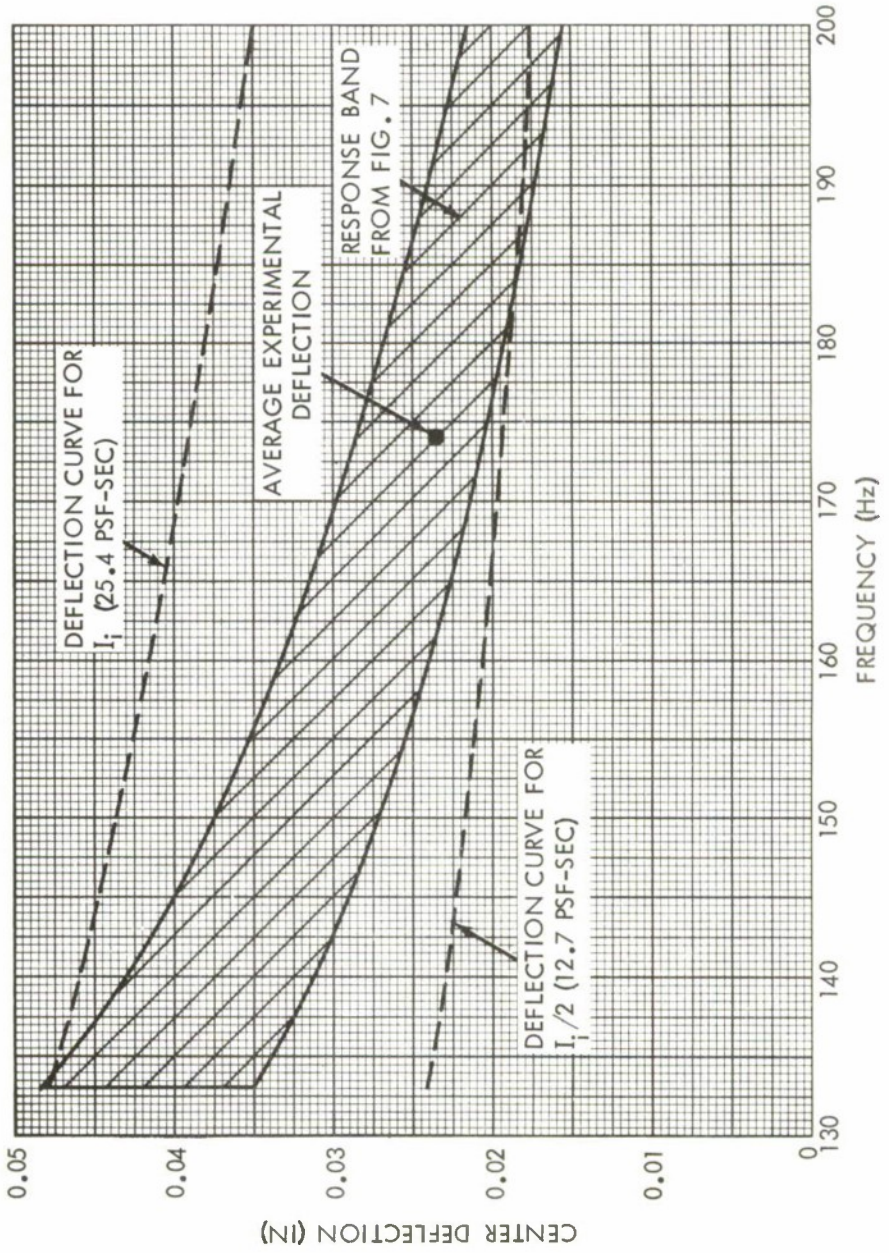

FIG. 10 COMPARISON OF IMPULSE-PREDICTED AND EXPERIMENTAL DEFLECTIONS

band from Figure 7. It is noted that this range of impulse encompasses the experimentally derived deflections. If significance is placed on the average deflection and frequency, we note that the prediction method based on I_i overestimated the deflection by 67 percent. Although the accuracy of this method is not overwhelming, an important objective has been accomplished. This elementary wall analysis with explosion impulse data from reference (2) does provide a conservative design basis for this type of construction. When one realizes that safety factors of from 2 to 10 are common in the design of safe explosion testing facilities, this simple analysis of a complex blast and stress problem takes on added significance.

Response to Gas Pressure. Thus far in the wall analysis we have dealt solely with the shock problem. Of equal concern for an enclosed explosion is the equilibrium static gas pressure that exists after the shock phenomena have subsided. To evaluate the wall stresses due to a static uniform load, we make use of Equations (36), (38), and (50). We find that the maximum tensile stress at the wall mid-height or center becomes

$$\sigma_c = 33.26\ Pb \left[- \frac{(3\ell^2 - b^2)}{6\ell} + \ell - b/2 \right] \qquad (60)$$

and the maximum tensile stress at the inside corner becomes

$$\sigma_B = 33.26\ Pb \left[- \frac{(3\ell^2 - b^2)}{6\ell} + \ell - b \right] \qquad (61)$$

Plots of these stresses for the three characteristic beam lengths are shown in Figure 11. We note for the gas pressure of 31.2 psi from the 5-lb pentolite explosion that all steel reinforcing stresses are well below the static yield. Also comparing these stresses with those shown in Figure 9 for the shock loading, we conclude that the shock loading is a more severe loading than the gas pressure for this particular construction and a pentolite explosion. However, the magnitude of the gas pressure is proportional to the heat of combustion of the explosive (see reference (4)). For pentolite the heat of combustion is 2.76 kcal/gm; for TNT it is 3.57. Then the gas pressure for 5 lb TNT might reach 40 psi. From Figure 9 we note that the wall center stress for 40-psi pressure is below the 40,000-psi static yield level. It is, however, sufficiently close to propose that the safe 5-lb TNT equivalent limit established for these bombproofs include equivalence of gas pressure as well as shock pressure and impulse. With the equivalent limit defined in this manner, venting the gas pressure is not necessary in these buildings.

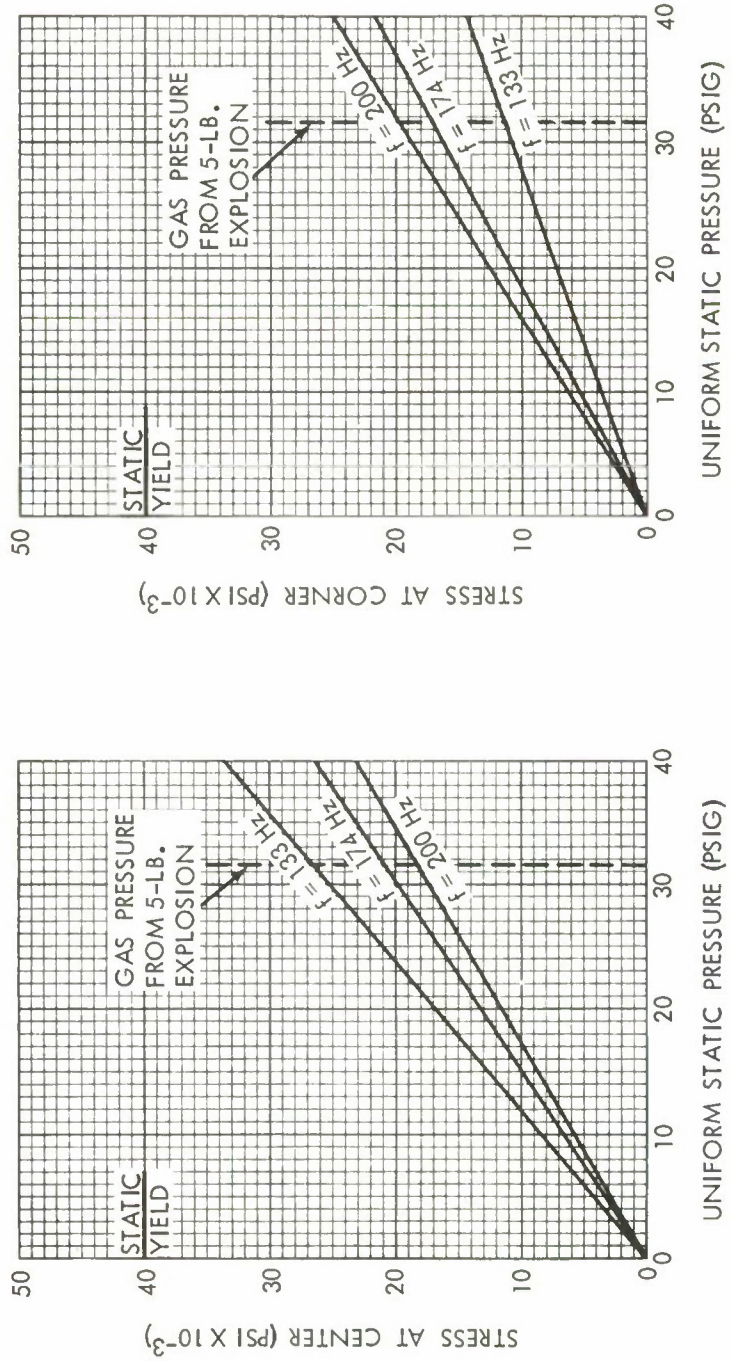

FIG. 11 WALL STRESSES FOR UNIFORM STATIC PRESSURE

CONCLUSIONS

The conclusions that can be drawn from this work fall into two categories: (1) information directly applicable to existing bombproofs at the Laboratory and (2) information germane to design criteria for future concrete explosion test facilities.

Existing Bombproofs. The external and internal blast data and the wall response data obtained from actual explosions in Building 324 provide the basis for the following conclusions.

1. The installation of heavy steel doors on existing bombproofs at the Laboratory should eliminate all noise and vibration complaints from neighboring private home owners to explosion testing at NOL. Airblast data showed that transmitted pressures from a 5-lb explosion in a completely closed bombproof were less than those produced by a $\frac{1}{2}$-lb charge with an open door -- actually the pressure level is less than that generated by a 1.5-gm TNT free-air explosion.

2. From internal gas pressure measurements and wall frequency response data, the assumed structural benefit of venting the explosion gases through existing bombproof labyrinth passageways has been shown to be a misconception. Because the slowest responding wall is still quite rapid (1.5-msec rise time), the wall views the gas pressure loading of even the fastest venting condition (160 msec) of an open passageway as though it were essentially a constant pressure.

3. A stress analysis of the concrete wall using experimentally derived wall deflections showed that the maximum stress in the reinforcing steel occurs at the wall mid-height and that this stress for a 5-lb pentolite explosion slightly exceeds the dynamic yield capacity of the wall. This explains the presence of cracks in the wall at the mid-height region. Even though the stress levels are just slightly above dynamic yield in this region for the 5-lb pentolite explosion, it is believed that there is no violation in safe firing limits based primarily on many years of firing at this level in these bombproofs. On the other hand, however, this study shows that the 5-lb TNT equivalent limit should not be exceeded in these buildings without the full knowledge that permanent structural damage could occur.

4. The definition of the safe 5-lb TNT equivalent explosive limit established for these bombproofs should include equivalence with respect to shock pressure, impulse, and gas pressure.

5. Within the defined explosive limit given in conclusion 4, the stress analysis showed that the shock loading produces greater wall stresses and deflections in these buildings than those generated by the static gas pressure from a 5-lb pentolite explosion. Thus the closure of the existing bombproofs should not create structural problems any more severe than those that currently exist.

With respect to the existing bombproofs at the Laboratory, there is no structural hazard involved in the installation of heavy steel doors in the labyrinth passageways. Because of the significant decrease in outside blast pressures afforded by a completely closed bombproof, the installation of such doors should be encouraged to increase test program efficiency and to eliminate neighbors' complaints. Increased exhaust system capacity in the bombproof and surrounding instrumentation rooms to remove post-test explosion gases more quickly would reduce the major inconvenience of conducting experiments with the closed door.

Design Criteria. This report, in addition to studying the experimental response of a particular bombproof, has presented simple methods of predicting response characteristics of concrete cubicle-type explosion testing facilities from available data on explosions.

1. Methods of predicting the explosion gas pressure in an enclosed space from references (2) and (4) were shown to adequately describe the maximum static overpressure. With this as input, the developed method of predicting the time to vent the explosion gases through a specified area has been shown to yield minimum vent times. These provide an adequate basis for determining whether the gas pressure loading should be considered as static or impulsive when building response is analyzed.

2. Shock loading in terms of average impulse on walls of cubicle-type construction appear to be conservatively estimated by curves presented in reference (2). The technique of converting the wall impulse to kinetic energy and equating this to wall strain energy provides a conservative model to predict wall stresses and deflections for elastic response. One advantage of this method is its use of "handbook" equations for moments, deflections, and stresses. However, sound engineering judgment is required in their use and manipulation.

The prediction methods developed here should provide a conservative design criteria for concrete cubicle-type structures similar to the bombproofs at NOL that are subjected to continuous explosion tests without suffering permanent damage or deterioration.

REFERENCES

1. C. N. Kingery, "Airblast Parameters Versus Distance for Hemispherical TNT Surface Bursts," Ballistic Research Laboratories, BRL Report No. 1344, September 1966

2. "Manual for Design of Protective Structures Used in Explosive Processing and Storage Facilities," prepared for DOD Armed Services Explosives Safety Board under the direction of Picatinny Arsenal by Amman & Whitney, review copy, to be published in 1969

3. E. Cohen, N. Dobbs, and R. Rindner, "Blast Pressures and Impulse Loads Produced by Explosions in Cubicle-Type Structures, Report No. 10, Establishment of Safety Design Criteria for Use in Engineering of Explosive Facilities and Operations," Picatinny Arsenal Technical Report 3604, May 1967

4. N. O. Holland (Editor), "Explosives - Effects and Properties," U. S. Naval Ordnance Laboratory, NOLTR 65-218, Confidential, February 1967

5. B. O. Peirce and R. M. Foster, A Short Table of Integrals, 4th edition, Ginn and Co., 1957

6. R. J. Roark, Formulas for Stress and Strain, 4th edition, McGraw-Hill, 1965

7. W. Flugge, Editor, Handbook of Engineering Mechanics, 1st edition, McGraw-Hill, 1962

8. S. Timoshenko and D. H. Young, Vibration Problems in Engineering, 3rd edition, D. Van Nostrand, 1955

9. G. Winter, L. C. Urquhart, C. E. O'Rourke, and A. H. Nilson, Design of Concrete Structures, 7th edition, McGraw-Hill, 1964

10. O. W. Eshbach, Editor, Handbook of Engineering Fundamentals, 2nd edition, John Wiley & Sons, 1952

11. F. E. Kidder and H. Parker, Kidder-Parker Architects' and Builders' Handbook, 18th edition, John Wiley & Sons, 1946

12. H. P. Tardif and W. Erickson, "The Experimental Properties of Metals Under Dynamic Loading," Canadian Armament Research and Development Establishment, CARDE Technical Memorandum No. 192/58, 1958

DISTRIBUTION LIST

	COPIES
CHIEF OF ENGINEERS, D/A WASHINGTON, D. C. 20310 ATTN: ENGCW-NE, ENGTE-E, ENGMC-E	3
COMMANDING OFFICER ABERDEEN PROVING GROUND ABERDEEN, MARYLAND 21005 ATTN: BRL FOR DIRECTOR, J. J. MESZAROS W. J. TAYLOR, R. E. SHEAR	2 2
COMMANDING GENERAL THE ENGINEER CENTER FT BELVOIR, VIRGINIA 22060 ATTN: ASST COMMANDANT, ENGINEER SCHOOL	
COMMANDING OFFICER PICATINNY ARSENAL DOVER, N. J. 07801 ATTN: SMUPA-G,-W,-VL,-VE,-VC,-DD -DR,-DR4,-DW,-TX,-TW,-V	6 6
DIRECTOR U. S. ARMY CORPS OF ENGINEERS WATERWAYS EXPERIMENT STATION VICKSBURG, MISSISSIPPI 39180 ATTN: LIBRARY, JOHN STRANGE	2
COMMANDING GENERAL WHITE SANDS MISSILE RANGE WHITE SANDS, NEW MEXICO 88002 ATTN: STEWS-AMTED-2	
CHIEF OF NAVAL OPERATIONS, NL WASHINGTON, D. C. 20350 ATTN: OP-75 OP-03EG	2 1

DEPARTMENT OF PHYSICS
STANFORD RESEARCH INSTITUTE
MENLO PARK, CALIFORNIA 94025
ATTN: MR. FRED M. SAUER

ITT RESEARCH INSTITUTE
ILLINOIS INSTITUTE OF TECHNOLOGY
10 WEST 35TH STREET
CHICAGO, ILLINOIS 60616

DENVER RESEARCH INSTITUTE
MECHANICS DIVISION, UNIVERSITY OF DENVER
DENVER, COLORADO 80210
ATTN: DR. RODNEY F. RECHT 2

DIRECTOR
APPLIED PHYSICS LABORATORY
JOHNS HOPKINS UNIVERSITY
8621 GEORGIA AVENUE
SILVER SPRING, MARYLAND 20910
ATTN: TECH LIBRARY

DDC
CAMERON STATION
ALEXANDRIA, VIRGINIA 22314
ATTN: TISIA-21 20

URS CORPORATION
1700 S. EL CAMINO REAL
SAN MATEO, CALIFORNIA 94401
ATTN: MR. KENNETH KAPLAN

HERCULES, INC.
ALLEGANY BALLISTICS LABORATORY
P. O. BOX 210
CUMBERLAND, MARYLAND 21502

SOUTHWEST RESEARCH INSTITUTE
8500 CULEBRA ROAD
SAN ANTONIO, TEXAS 78206
ATTN: DR. ROBERT C. DEHART

BATTELLE MEMORIAL INSTITUTE
505 KING AVENUE
COLUMBUS, OHIO 43201
ATTN: MR. R. W. KLINGENSMITH
VIA: ADVANCED RESEARCH PROJECTS AGENCY
THE PENTAGON, WASHINGTON, D. C. 20390

COMMANDER
NAVAL AIR SYSTEMS COMMAND
WASHINGTON, D. C. 20360
ATTN: AIR-604
-350
-52023

COMMANDER
NAVAL SHIP SYSTEMS COMMAND
WASHINGTON, D. C. 20360
ATTN: SHIP-2021
-6423

COMMANDER
NAVAL WEAPONS CENTER
CHINA LAKE, CALIFORNIA 93555
ATTN: LIBRARY, R. E. BOYER, DR. MALLORY 3

COMMANDING OFFICER AND DIRECTOR
U. S. NAVAL CIVIL ENGINEERING LABORATORY
PORT HUENEME, CALIFORNIA 93041
ATTN: CODE L31

DIRECTOR
U. S. NAVAL RESEARCH LABORATORY
WASHINGTON, D. C. 20390
ATTN: LIBRARY
DR. LOUIS F. DRUMMETER

COMMANDING OFFICER AND DIRECTOR
NAVAL SHIP RESEARCH AND DEVELOPMENT CENTER
WASHINGTON, D. C. 20007
ATTN: LIBRARY

UNDERWATER EXPLOSIONS RESEARCH DIVISION
NAVAL SHIP RESEARCH AND DEVELOPMENT DIVISION
PORTSMOUTH, VIRGINIA 23709

COMMANDER
U. S. NAVAL WEAPONS EVALUATION FACILITY
KIRTLAND AFB, NEW MEXICO 87117
ATTN: LIBRARY, [WEVS] 2

COMMANDING OFFICER
U. S. NAVAL ORDNANCE STATION
INDIAN HEAD, MARYLAND 20640
ATTN: LIBRARY

COMMANDER
U. S. NAVAL WEAPONS LABORATORY
DAHLGREN, VIRGINIA 22448
ATTN: TERMINAL BALLISTICS DEPARTMENT 1
TECHNICAL LIBRARY 2

DIRECTOR OF CIVIL ENGINEERING
HQ USAF
WASHINGTON, D. C 20330
ATTN: AFOCE

COMMANDER
TEST COMMAND, DEFENSE ATOMIC SUPPORT AGENCY
SANDIA BASE, ALBUQUERQUE, NEW MEXICO 87115
ATTN: FCWT, FCTG 2

DIRECTOR
DEFENSE ATOMIC SUPPORT AGENCY
WASHINGTON, D. C. 20305
ATTN: SPLN, SPAS, **LIBRARY** 3

DIRECTOR
U. S. BUREAU OF MINES
DIVIDION OF EXPLOSIVE TECHNOLOGY
4800 FORBES STREET
PITTSBURGH, PENNSYLVANIA 15213
ATTN: DR. ROBERT W. VAN DOLAH

CHAIRMAN
ARMED SERVICES EXPLOSIVES SAFETY BOARD
NASSIF BLDG., 5616 COLUMBIA PIKE
WASHINGTON, D. C. 20315
ATTN: MR. R. G. PERKINS

E. I. duPont de Nemours & Company
Eastern Laboratory
Explosives Department
Gibbstown, New Jersey 08027
ATTN: Dr. L. Coursen

Director
Los Alamos Scientific Laboratory
P. O. Box 1663
Los Alamos, New Mexico 87544
ATTN: Library

Commander
Eglin Air Force Base
Florida 32542
ATTN: DET. 4, ASD Weapons Division
ASQWR (Mr. Kyselka)

Ammann & Whitney
111 8th Avenue
New York, N. Y. 10011

Commander
AFWL (WLIL)
Kirtland Air Force Base
New Mexicc 87117

President
Sandia Corporation, Sandia Base
Albuquerque, New Mexico 87115
ATTN: Dr. M. L. Merritt
W. B. Bendick
W. Roberts
J. W. Reed
Dr. C. Broyles

Sandia Corporation
Livermore Laboratory
P. O. Box 969
Livermore, California 94550

University of California
Lawrence Radiation Laboratory
P. O. Box 808
Livermore, California 94550
ATTN: Tech Info Div, Dr. Joseph B. Knox 2

Commanding Officer and Director
U. S. Naval Civil Engineering Laboratory
Port Hueneme, California 93041
ATTN: Code L31

Commander
Naval Ordnance Systems Command
Washington, D. C. 20360
ATTN: B. E. Drimmer - ORD-033
Dr. A. B. Amster - ORD-0332
M. F. Murphy - ORD-03323
H. M. Roylance - ORD-932

Commander
Naval Material Command
Washington, D. C. 20360
ATTN: I. Jaffee - MAT 0312D
T. A. Kleback MAT-0332
G. T. Swiggum MAT-03322

Director of Navy Laboratories
Department of the Navy
Washington, D. C. 20360
ATTN: NMAT-03L

Commander
Naval Facilities Engineering Command
Washington, D. C. 20510
ATTN: Facilities Planning NFAC-20
Officer-in-Charge of Chesapeake
Division of Naval Facilities Engineering Command

UNCLASSIFIED

Security Classification

DOCUMENT CONTROL DATA - R&D

(Security classification of title, body of abstract and indexing annotation must be entered when the overall report is classified)

1. ORIGINATING ACTIVITY (Corporate author)	2a. REPORT SECURITY CLASSIFICATION
U. S. Naval Ordnance Laboratory White Oak, Silver Spring, Maryland 20910	UNCLASSIFIED
	2b. GROUP

3. REPORT TITLE

STRUCTURAL ANALYSIS OF NOL EXPLOSION TESTING FACILITIES

4. DESCRIPTIVE NOTES (Type of report and inclusive dates)

5. AUTHOR(S) (Last name, first name, initial)

Proctor, James F.

6. REPORT DATE	7a. TOTAL NO. OF PAGES	7b. NO. OF REFS
24 April 1969	40	12

8a. CONTRACT OR GRANT NO.	9a. ORIGINATOR'S REPORT NUMBER(S)
b. PROJECT NO.	TR 69-84
c.	9b. OTHER REPORT NO(S) (Any other numbers that may be assigned this report)
d.	

10. AVAILABILITY/LIMITATION NOTICES

This document is subject to special export controls and each transmittal to foreign government or foreign nationals may be made only with prior approval of NOL.

11. SUPPLEMENTARY NOTES	12. SPONSORING MILITARY ACTIVITY

13. ABSTRACT

Installation of a heavy steel door in the labyrinth passageway of existing Naval Ordnance Laboratory explosion testing facilities (bombproofs) is shown to reduce drastically the transmitted airblast pressure outside the building. Completely enclosing an explosion in this manner has caused concern for the structural capability of the bombproofs to withstand both the shock pressures and long duration gas pressures on a continuous use basis. This report presents an experimental and analytical study of the structural response of a typical bombproof to contained and vented explosions. It shows that the maximum deflections and stresses in the building are not significantly altered by completely enclosing the explosion. Experimental blast and response data are presented and compared with analytical predictions.

DD FORM 1 JAN 64 1473

UNCLASSIFIED

Security Classification

14. KEY WORDS	LINK A		LINK B		LINK C	
	ROLE	WT	ROLE	WT	ROLE	WT
Explosion Response Explosion Test Facility Confined Explosions Structural Response Concrete Wall Response Response Design						

INSTRUCTIONS

1. ORIGINATING ACTIVITY: Enter the name and address of the contractor, subcontractor, grantee, Department of Defense activity or other organization *(corporate author)* issuing the report.

2*a*. REPORT SECURITY CLASSIFICATION: Enter the overall security classification of the report. Indicate whether "Restricted Data" is included. Marking is to be in accordance with appropriate security regulations

2*b*. GROUP: Automatic downgrading is specified in DoD Directive 5200.10 and Armed Forces Industrial Manual. Enter the group number. Also, when applicable, show that optional markings have been used for Group 3 and Group 4 as authorized.

3. REPORT TITLE: Enter the complete report title in all capital letters. Titles in all cases should be unclassified. If a meaningful title cannot be selected without classification, show title classification in all capitals in parenthesis immediately following the title.

4. DESCRIPTIVE NOTES: If appropriate, enter the type of report, e.g., interim, progress, summary, annual, or final. Give the inclusive dates when a specific reporting period is covered.

5. AUTHOR(S): Enter the name(s) of author(s) as shown on or in the report. Enter last name, first name, middle initial. If military, show rank and branch of service. The name of the principal author is an absolute minimum requirement.

6. REPORT DATE: Enter the date of the report as day, month, year; or month, year. if more than one date appears on the report, use date of publication.

7*a*. TOTAL NUMBER OF PAGES: The total page count should follow normal pagination procedures, i.e., enter the number of pages containing information.

7*b*. NUMBER OF REFERENCES: Enter the total number of references cited in the report.

8*a*. CONTRACT OR GRANT NUMBER: If appropriate, enter the applicable number of the contract or grant under which the report was written.

8*b*, 8*c*, & 8*d*. PROJECT NUMBER: Enter the appropriate military department identification, such as project number, subproject number, system numbers, task number, etc.

9*a*. ORIGINATOR'S REPORT NUMBER(S): Enter the official report number by which the document will be identified and controlled by the originating activity. This number must be unique to this report.

9*b*. OTHER REPORT NUMBER(S): If the report has been assigned any other report numbers *(either by the originator or by the sponsor)*, also enter this number(s).

10. AVAILABILITY/LIMITATION NOTICES: Enter any limitations on further dissemination of the report, other than those imposed by security classification, using standard statements such as:

(1) "Qualified requesters may obtain copies of this report from DDC."

(2) "Foreign announcement and dissemination of this report by DDC is not authorized."

(3) "U. S. Government agencies may obtain copies of this report directly from DDC. Other qualified DDC users shall request through

_____."

(4) "U. S. military agencies may obtain copies of this report directly from DDC. Other qualified users shall request through

_____."

(5) "All distribution of this report is controlled. Qualified DDC users shall request through

_____."

If the report has been furnished to the Office of Technical Services, Department of Commerce, for sale to the public, indicate this fact and enter the price, if known.

11. SUPPLEMENTARY NOTES: Use for additional explanatory notes.

12. SPONSORING MILITARY ACTIVITY: Enter the name of the departmental project office or laboratory sponsoring *(paying for)* the research and development. Include address.

13. ABSTRACT: Enter an abstract giving a brief and factual summary of the document indicative of the report, even though it may also appear elsewhere in the body of the technical report. If additional space is required, a continuation sheet shall be attached.

It is highly desirable that the abstract of classified reports be unclassified. Each paragraph of the abstract shall end with an indication of the military security classification of the information in the paragraph, represented as *(TS)*, *(S)*, *(C)*, or *(U)*.

There is no limitation on the length of the abstract. However, the suggested length is from 150 to 225 words.

14. KEY WORDS: Key words are technically meaningful terms or short phrases that characterize a report and may be used as index entries for cataloging the report. Key words must be selected so that no security classification is required. Identifiers, such as equipment model designation, trade name, military project code name, geographic location, may be used as key words but will be followed by an indication of technical context. The assignment of links, roles, and weights is optional.